Video Article

Modeling Mucosal Candidiasis in Larval Zebrafish by Swimbladder Injection

Remi L. Gratacap[1], Audrey C. Bergeron[1], Robert T. Wheeler[1,2]

[1]Department of Molecular and Biomedical Sciences, University of Maine

[2]Graduate School of Biomedical Sciences and Engineering, University of Maine

Correspondence to: Robert T. Wheeler at robert.wheeler@umit.maine.edu

URL: http://www.jove.com/video/52182
DOI: doi:10.3791/52182

Keywords: Immunology, Issue 93, Zebrafish, mucosal candidiasis, mucosal infection, epithelial barrier, epithelial cells, innate immunity, swimbladder, *Candida albicans*, *in vivo*.

Date Published: 11/27/2014

Citation: Gratacap, R.L., Bergeron, A.C., Wheeler, R.T. Modeling Mucosal Candidiasis in Larval Zebrafish by Swimbladder Injection. *J. Vis. Exp.* (93), e52182, doi:10.3791/52182 (2014).

Abstract

Early defense against mucosal pathogens consists of both an epithelial barrier and innate immune cells. The immunocompetency of both, and their intercommunication, are paramount for the protection against infections. The interactions of epithelial and innate immune cells with a pathogen are best investigated *in vivo*, where complex behavior unfolds over time and space. However, existing models do not allow for easy spatio-temporal imaging of the battle with pathogens at the mucosal level.

The model developed here creates a mucosal infection by direct injection of the fungal pathogen, *Candida albicans*, into the swimbladder of juvenile zebrafish. The resulting infection enables high-resolution imaging of epithelial and innate immune cell behavior throughout the development of mucosal disease. The versatility of this method allows for interrogation of the host to probe the detailed sequence of immune events leading to phagocyte recruitment and to examine the roles of particular cell types and molecular pathways in protection. In addition, the behavior of the pathogen as a function of immune attack can be imaged simultaneously by using fluorescent protein-expressing *C. albicans*. Increased spatial resolution of the host-pathogen interaction is also possible using the described rapid swimbladder dissection technique.

The mucosal infection model described here is straightforward and highly reproducible, making it a valuable tool for the study of mucosal candidiasis. This system may also be broadly translatable to other mucosal pathogens such as mycobacterial, bacterial or viral microbes that normally infect through epithelial surfaces.

Video Link

The video component of this article can be found at http://www.jove.com/video/52182/

Introduction

Mucosal infections can lead to life threatening bloodstream infections due to the damage of the epithelial barrier, which allows pathogens access to the systemic environment[1,2]. In addition, mucosal infections can also cause significant immunopathology even when contained externally[3-5]. The commensal unicellular fungus *Candida albicans* is present in the majority of the population in the oral cavity and other mucosal sites[6-9]. Although normally contained by innate and adaptive immune responses, innate immune defects and medical interventions can lead to severe mucosal candidiasis. The assault on the epithelial barrier results in an increased risk of life threatening disseminated disease as well as immunopathology, as in the case of vulvo-vaginal candidiasis, additionally *C. albicans* colonization has been linked with lung immune homeostasis[10,11]. Disseminated candidiasis is now the fourth most common bloodstream infection in intensive care units[12] and mortality as high as 40% makes it a major concern. Due to the increase in immunomodulatory treatments for patients with autoimmune diseases, cancer or organ transplants, it is imperative to understand the interaction between this pathogen and the mucosal immune compartment.

The majority of cell biological advances regarding *C. albicans*-cell interactions at the mucosal level come from *in vitro*[13-15] and murine models[16-18]. Both these approaches have distinct advantages, but the ability to image live cells at high resolution in an intact host has limited the temporal and spatial characterization of the infection. For these studies, there is the need for an *in vivo* model where the interaction of pathogen, innate immune and epithelial cells can be visualized in an intact vertebrate host.

The zebrafish has emerged as an invaluable tool for the understanding of human disease, mainly due to its transparency and amenability to genetic manipulation. Cell and organ development have been imaged in exquisite detail, which has led to the description of novel immune cell behaviors, such as T cell behavior in the developing thymus[19] or the battle between intracellular mycobacteria and phagocytes[20-22]. Recent work has described intestinal microbe-host interactions in zebrafish and shown that microbial colonization of the intestinal tract affects host intestinal physiology and resistance to other infections[23,24]. Furthermore, infection through the gut epithelium has been described for several pathogens.

In contrast to the intestinal tract, the swimbladder represents a more isolated and complementary mucosal model. This organ is an extension of the developing gut tube and forms anteriorly to the liver and pancreas[25,26]. It produces surfactant, mucus and antimicrobial peptides[27,28] and anatomically, as well as ontogenetically, this organ is considered a homologue of the mammalian lung[29,30]. Since the pneumatic duct remains

connected to the gut in the zebrafish, this allows for immersion infection to occur naturally. Remarkably, the only known naturally occurring infections of fish with *Candida* species are *C. albicans* infections in the swimbladder[31]. We recently described an experimental immersion infection model where *C. albicans* infects the swimbladder, and found that this infection recapitulates some of the hallmarks of *C. albicans*-epithelial interaction *in vitro*[32,33].

In the method presented here, the original immersion infection model is improved by directly injecting *C. albicans* into the swimbladder of 4 days post fertilization (dpf) zebrafish. This allows for precise temporal control of infection as well as a highly reproducible inoculum. It permits detailed intravital imaging, coupled with the versatility of the zebrafish model. As an example of what can be done with this method, we present the spatio-temporal dynamics of *C. albicans* growth along with neutrophil recruitment to the site of infection. Because zebrafish swimbladder tissue is challenging to image intravitally, we also present a rapid swimbladder dissection technique that improves fluorescence signal and microscopic resolution. These methods expand the toolbox for fungal, immunological, and aquaculture research as well as describing a novel infection route that may be translated to model other fungal, bacterial or viral infections of mucosal surfaces.

Protocol

NOTE: All zebrafish care protocols and experiments were performed in accordance with NIH guidelines under Institutional Animal Care and Use Committee (IACUC) protocol A2012-11-03.

1. Zebrafish Rearing to 4 Days Post Fertilization

1. Collect AB zebrafish, or any other transgenic lines, within the first 3 hr post fertilization, as shown in another video[34].
2. Incubate 120 eggs in a 15 cm Petri dishes containing 150 ml of E3 media (5 mM NaCl; 0.17 mM KCl; 0.33 mM $CaCl_2$; 0.33 mM $MgCl_2$; 2 mM HEPES; pH 6.8) with methylene blue (0.3 µg/ml final concentration) in a 33 °C incubator with 12/12 light/dark photoperiod.
3. Replace the media after 6 hr with E3 + PTU (1-phenyl-2-thiourea, 10 µg/ml final concentration) and remove the dead eggs.
4. Incubate for 4 days at 33 °C, exchanging the media with fresh E3 + PTU after 2 days.

2. Injection Micro-needle Preparation

1. Pull borosilicate capillary (OD 1.2 mm; ID 0.69 mm) into a micro-needle using a needle puller with the following settings (550 Heat; 0 Pull; 130 Velocity; 110 Time).
   NOTE: The settings will vary from filament to filament to obtain similarly shaped micro-needles (see **Figure 1**) and will need to be readjusted whenever a new filament is installed.
2. Fill a micro-needle with 3 µl of 0.4 µm-filtered phosphate buffer saline (PBS; 137 mM NaCl; 2.7 mM KCl; 10 mM Na_2HPO_4; 1.8 mM KH_2PO_4; pH 7.4) using a 20 µl microloader pipette tip.
3. Set up the micro-needle on a micropipette holder on a micromanipulator attached to a pressure injection system. Set the injection pressure to 30 PSI and the pulse duration at 30 msec.
4. Using a Petri dish with distilled water, lower the micro-needle until 1/5 of the needle is in the water. Clip the micro-needle with fine tweezers just below the water level. Bring the micro-needle out of the water and push the pedal several times until a bolus appears.
5. Measure the diameter of the bolus by lowering the micro-needle on a hemocytometer layered with one drop of type A immersion oil. Adjust the pulse duration to obtain the desired volume (see **Table 1**).
6. Set the backpressure for the bolus to remain stable in oil (lower the pressure if the bolus increases volume and increase the backpressure if the bolus volume decreases). Record the pulse duration for each micro-needle.
7. Remove the PBS from the micro-needle by aspirating it using a microloader pipette tip and expel the left-over PBS by placing it back on the injector and flipping the continuous pulse switch. Reserve each micro-needle.

3. *Candida* Preparation

1. Streak *Candida albicans* transformed with codon-optimized dTomato, GFP, BFP, EOS or Far Red from a frozen stock (-80 °C stock in 25% glycerol) using a sterile wooden dowel onto a yeast peptine dextrose (YPD) agar plate (10 g/L yeast extract, 20 g/L peptone, 20 g/L dextrose, 20 g/L agar; autoclaved and poured 25 ml in Petri dishes) and incubate overnight at 30 °C.
2. Pick one colony using a sterile wooden dowel and inoculate to 5 ml of YPD liquid (10 g/L yeast extract, 20 g/L peptone, 20 g/L dextrose, autoclaved and aseptically aliquotted in 5 ml in 16 x 150 mm glass culture tubes).
3. Incubate overnight at 30 °C in a roller drum at 60 rpm.
4. Collect 1 ml of *C. albicans* culture and transfer into a 1.7 ml sterile centrifuge tube.
5. Centrifuge at 5,000 x g for a couple of sec. Empty the supernatant and add 1 ml of sterile PBS, vortex thoroughly. Repeat this twice.
6. Count the colonies using a hemocytometer by diluting the 1 ml stock 1:1,000 in sterile PBS.

4. Injecting Zebrafish in the Swimbladder

1. Warm an injection dish (2% agarose) for 30 min in a 33 °C incubator.
2. At the desired time, remove 100 of the 150 ml of E3 + PTU from the 15 cm Petri dish containing the fish to inject using a 25 ml pipette without aspirating any zebrafish.
3. Anesthetize 4 dpf zebrafish by adding 2 ml of a 4 mg/ml buffered tricaine methane sulfonate stock (TR) to the 50 ml media remaining (final concentration 200 µg/ml) and wait for 15 min.
4. Under a dissecting microscope, select fish with an inflated swimbladder. Fish can also be screened at that time for homogenous phenotype, such as neutrophil distribution in *mpo:GFP* line using an epifluorescence dissecting microscope.
5. Dilute the *C. albicans* stock from its original concentration (**step 3.8**) to 1.5 x 10^7 colony forming units per ml (cfu/ml) in PBS.

6. Transfer 30 zebrafish onto the injection dish using a plastic transfer pipette and remove the excess media.
7. Using a fishing-wire tool (0.012 inch diameter fishing line super-glued into a borosilicate capillary), make 3 lines of 10 fish, by holding the injection dish vertically and orientate the fish vertically.
8. Remove the excess media.
9. Thoroughly vortex the tube with 1.5 x 10^7 cfu/ml *C. albicans*.
10. Fill one micro-needle with 3 µl of *C. albicans* using a new microloader pipette tip and set the pulse duration to the appropriate setting (see **step 2.9**).
11. Rotate the injection dish to make an angle of 20° between the micro-needle and the head of the fish, aiming toward the back of the swimbladder (**Figure 3A**).
12. Push the micro-needle into the swimbladder, making sure the bore of the needle is in the lumen, and press the pedal once.
13. Repeat for each fish and transfer to a recovery dish (25 ml E3 + PTU) by flooding the dish with E3 and emptying it into the recovery dish.
14. Transfer another 30 fish to the injection dish.
15. Repeat injection with a new micro-needle filled with thoroughly vortexed *C. albicans*.
16. Finish by injecting the PBS control, if necessary, using a different injection dish to avoid contamination and transfer to a separate recovery dish (**step 4.10**).

5. Screening the Fish for Desired Inoculum

1. Prepare 40 ml of 0.4% low-melt agarose solution (LMA) by adding 160 mg of low melt agarose to 40 ml of E3, boiling by microwaving until dissolved, and cooling to 37 °C. Add 400 µl of TR (final concentration 200 µg/ml) once cooled.
2. After 30 min recovery, anaesthetize the fish as described (**step 4.3** using only 1 ml of TR into 25 mL E3 + PTU, final concentration 200 µg/ml).
3. Transfer 30 fish (with as little media as possible) to 2 ml of LMA in a weight boat.
4. Aspirate individual fish with a transfer pipette and plate the fish with 1 drops of LMA into a 96-well imaging plate, using only the 10 x 6 central wells.
5. Repeat until all the fish to screen are loaded to the imaging plate.
6. Let the media solidify at room temperature for 5 min.
7. Position the fish on their side, making sure they are in contact with the glass bottom.
8. Using the 20X objective on an inverted epifluorescence/confocal microscope and the appropriate filter, record the number of *C. albicans* yeast cells in each fish's swimbladder.
9. Select the fish with 15-25 yeast cells in the swimbladder (or desired inoculum), euthanize non-selected fish (800 µg/ml of TR in E3) and return selected fish to a deep Petri dish with 50 ml of E3 + PTU by adding 3 drops of E3 to the imaging plate selected wells and aspirating the fish with a plastic transfer pipette.
10. Incubate at 33 °C for the desired duration.

6. Imaging the Fish Post-screening

1. At the desired time, remove 25 of the 50 ml of E3 + PTU media from the deep Petri dish containing the fish to image.
2. Anaesthetize the fish as described (**step 4.3** using only 1 ml of TR into 25 ml E3 + PTU remaining, final concentration 200 µg/ml).
3. Plate the fish into a 96-well imaging plate and position appropriately (**steps 5.3 - 5.7**).
4. Image by scanning confocal microscopy using the appropriate lasers and emission filters. First focus on the fish using the 4X objective under differential interference contrast (DIC) and acquire images of the region of interest using the 20X objective with the confocal lasers in scanning mode with 2 µsec/pixel speed and 1024 x 600 pixel aspect ratio. Acquire Z-stacks with 1 µm step size, applying Kalman filter mode of 3 frames.
5. Return to a deep Petri dish with 50 ml E3 + PTU or into individual wells (24-well culture dish, 3 ml E3 + PTU) and incubate at 33 °C.

7. Dissecting the Swimbladder

1. Fill a 10 ml syringe with high vacuum grease.
2. Prepare a 2% LMA (**step 5.3** with 160 mg of low melting agarose in 8 ml of E3).
3. At the desired time, anaesthetize the fish (**step 5.2**).
4. Transfer 10 fish to a 1.7 ml centrifuge tube with 1 ml of E3 and euthanize by adding 200 µl of 4 mg/ml Tricaine (final concentration 800 µg/ml) to the centrifuge tube and incubating for 15 min at room temperature.
5. Prepare an imaging glass slide by placing 4 drops of vacuum grease in a square, 1 cm apart on a microslide (75 x 25 mm, **Figure 2**).
6. Place 2 drops of 2% LMA in the middle of the square.
7. Place one fish on a separate glass slide under a dissecting microscope and verify that the heart has stopped beating, remove the excess water.
8. Using fine tweezers dissect the swimbladder by maintaining the head in a fixed position with the left tweezers and pulling down the anterior gut with the right tweezers (**Figure 4A**).
9. Pick up the swimbladder by the pneumatic duct with the left tweezers, separating it from the digestive tract, and place it at the center of the 2% LMA before it solidifies.
10. Place a cover-slip (18 x 18 mm) on top of the imaging glass slide and push it until it touches the vacuum grease as well as the LMA (**Figure 2**).
11. Image within 10 min of dissection as described in **step 6.4**. Repeat **step 7.7 - 7.11** with the other fish.

Representative Results

Microinjection in the posterior swimbladder

The experimental method presented here describes the injection of a consistent dose of *C. albicans* yeast cells in the swimbladder of 4 dpf zebrafish. Previous work with the immersion model suggests that the swimbladder immune response to *C. albicans* is similar to mammalian mucosal candidiasis[32]. Here we demonstrate a modified infection method that is more straightforward, reproducible and rapid; several hundreds of zebrafish can be injected and screened within a couple of hours.

Accurate and reproducible infection of the swimbladder is accomplished by targeting the posterior area of the organ by microinjection. Injection into the swimbladder is easier to learn than most other microinjection routes for the larval or embryonic zebrafish (*e.g.,* intravenous or hindbrain ventricle). The preparation of the fish before injection is similar to that for other injection sites, with the exception that the swimbladder needs to be inflated so the fish are older. Approximately 75% of the fish raised at 33 °C have an inflated swimbladder by 4 dpf (data not shown). The swimbladder is located under an epidermal as well as thin muscle layer and the micro-needle used for injecting the fish needs to be beveled. The angle at which the fish are injected (**Figure 3A**) also greatly improves the speed and ease of the procedure. Injection of the bolus at the back of the swimbladder is important as it allows visualization of all the yeast cells when screening and avoids the presence of yeast cells on each side of the swimbladder, which will skew the selection range. Injecting toward the back of the swimbladder also avoids a possible loss of the inoculum through the pneumatic duct and then down the digestive tract. Verifying which fish has been injected is relatively easy as the bolus displaces the air bubble and the back of the swimbladder is subsequently filled with media (**Figure 3C**). It is also possible to use phenol red when injecting, which will make the visualization easier. Because of the size of *C. albicans* yeast cells (3 - 4 µm), the inoculum dose is limited to concentrations below 5 x 10^7 cfu/ml due to clogging of the micro-needle. This allows the injection of between one and 250 yeast cells within a 5 nl bolus. In our hands, injecting 4 nl at 1-1.5 x 10^7 cfu/ml gave the most consistent results. This resulted in a range of 10-50 yeast cells per fish. Narrowing the inoculum to 15-25 yeast cells (**Figure 3B**) gives a tighter phenotype and response. Using these conditions, approximately 50% of the fish injected have the appropriate inoculum range with over 95% survival 24 hr post injection (data not shown). It is also possible to keep fish with a lower/higher inoculum in order to investigate the effect of pathogen burden on disease development.

The swimbladder is approximately 100 nl total volume (400 x 200 x 200 µm, L x H x W, using the formula for the volume of an ellipsoid) so injection of higher volumes is also possible (up to 3 pulses of 4 nl have been used without any significant effect on the survival of the fish; data not shown).

Longitudinal intravital imaging of individual fish to follow both host and pathogen behavior

The behavior of both host and pathogen can be followed non-invasively for several days using this model. The ability to image the development of the infection at high resolution *in vivo* can and has been used to examine the pathogenesis of mucosal candidiasis. Neutrophils play a key role in resistance to candidiasis in mice and humans[35-38]. Using *mpo:GFP* zebrafish[39] (neutrophils express green fluorescent protein), and *C. albicans* expressing the dTomato red fluorescent protein[32], we have observed neutrophil-*Candida* dynamics during early infection (**Figure 4**).

Neutrophils are the first innate cell type to be recruited to the site of mucosal infection, and the infection of the swimbladder with live *C. albicans* leads to a rapid and continuous recruitment of neutrophils (**Figure 4A, B**). Interestingly, neutrophils are not substantially recruited to the swimbladder when heat-killed yeast cells were injected (**Figure 4A, B**).

Filaments develop rapidly after injection of yeast cells and *C. albicans* continues to germinate for the first 48 hr post injection (hpi). However, after this point the number of filaments decreases (**Figure 4D**) and the proportion of yeast increases (not shown). The ability to follow individual fish non-invasively enables these longitudinal studies (24-well plate tissue culture dishes) and highlights the individual differences in disease progression and host responses (**Figure 4C**). Such detailed studies enumerating fungal and immune cells at the site of infection over several days remain impractical in the mouse.

A rapid swimbladder dissection technique to improve imaging

Imaging the interaction of immune or epithelial cells with *C. albicans* is relatively easy in the model presented here. However, in certain circumstances, the presence of the air bubble and the thickness of the tissue surrounding the swimbladder, skin and muscles, compromises detailed spatial resolution. To improve image quality we have developed a method to dissect the swimbladder out of the zebrafish and image it rapidly (within 10 min) by confocal microscopy (**Figure 5A**). This is particularly useful when imaging transgenic fish lines where the fluorescence is ubiquitously expressed and there is extraneous fluorescence in the surrounding tissue, such as NF-κB:GFP[40] or α-catenin:citrine lines[41,42] (**Figure 5B, C**). The technique requires dexterity and practice to perform rapidly, but it is feasible to completely image 95% of all the fish attempted.

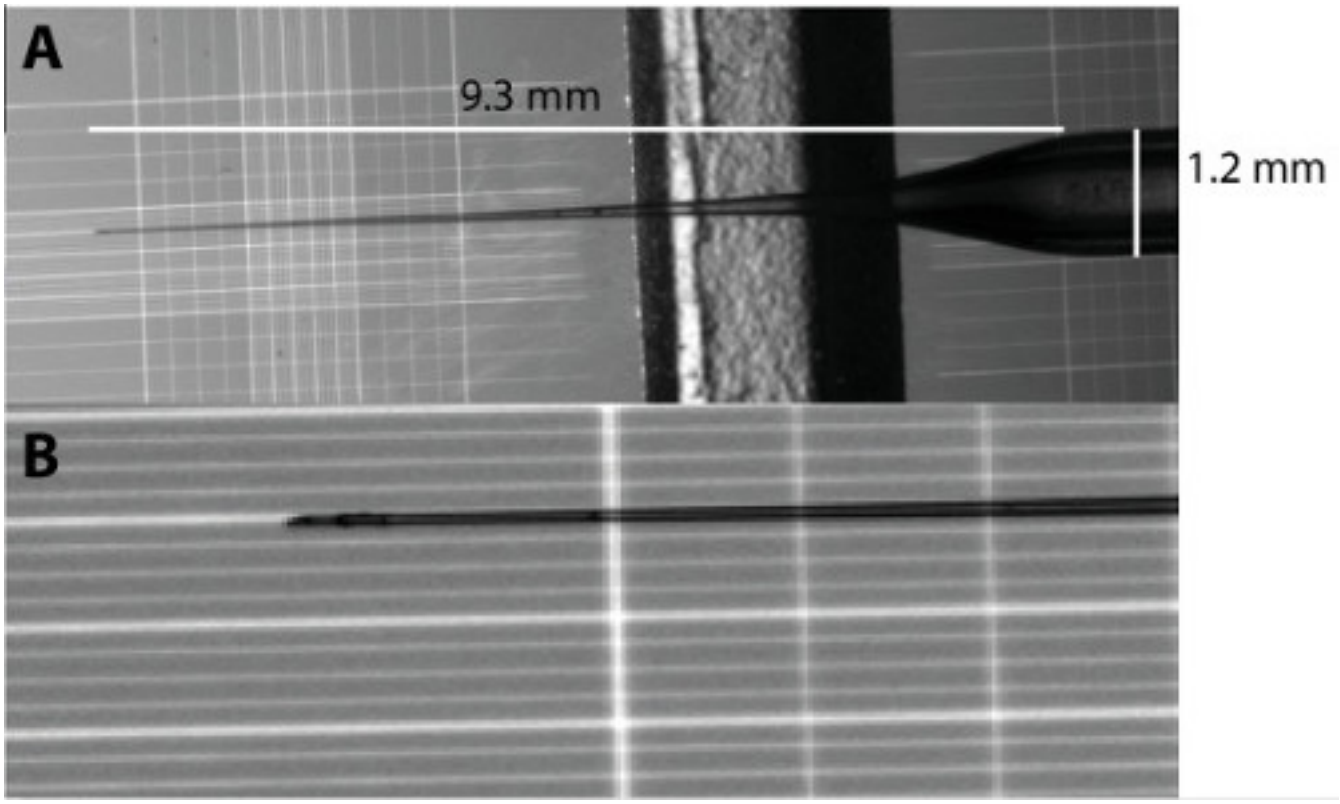

Figure 1: Micro-needle shape for swimbladder injection. (A) Overview of the micro-needle shape and measurement. **(B)** Magnification of the micro-needle tip from A. Each major vertical line in B are 0.2 mm apart.

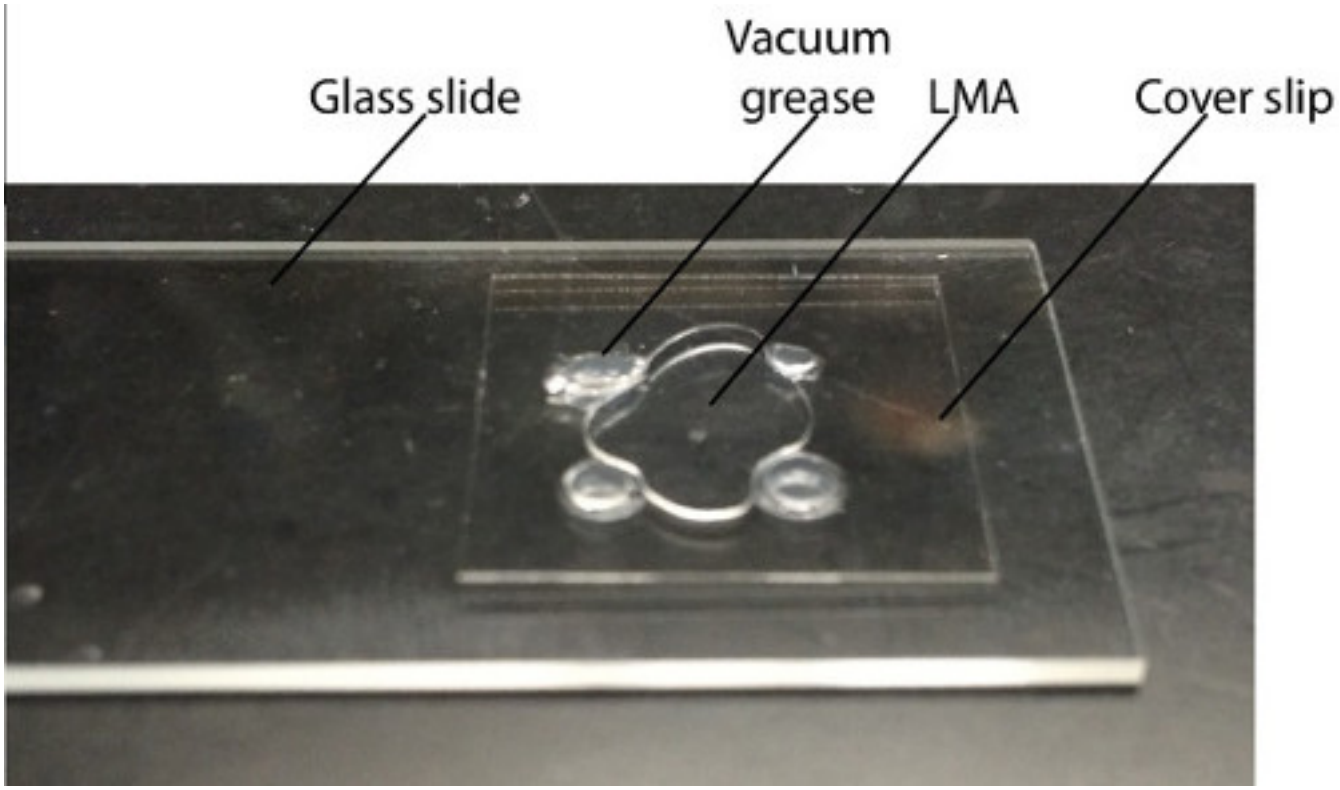

Figure 2: Imaging slide. A 2% LMA drop is placed in the middle of 4 dots of vacuum grease, 1 cm apart on a glass slide. The dissected swimbladder is placed in the middle of the LMA and a cover slip is lowered on top until it makes contact with the LMA and the vacuum grease.

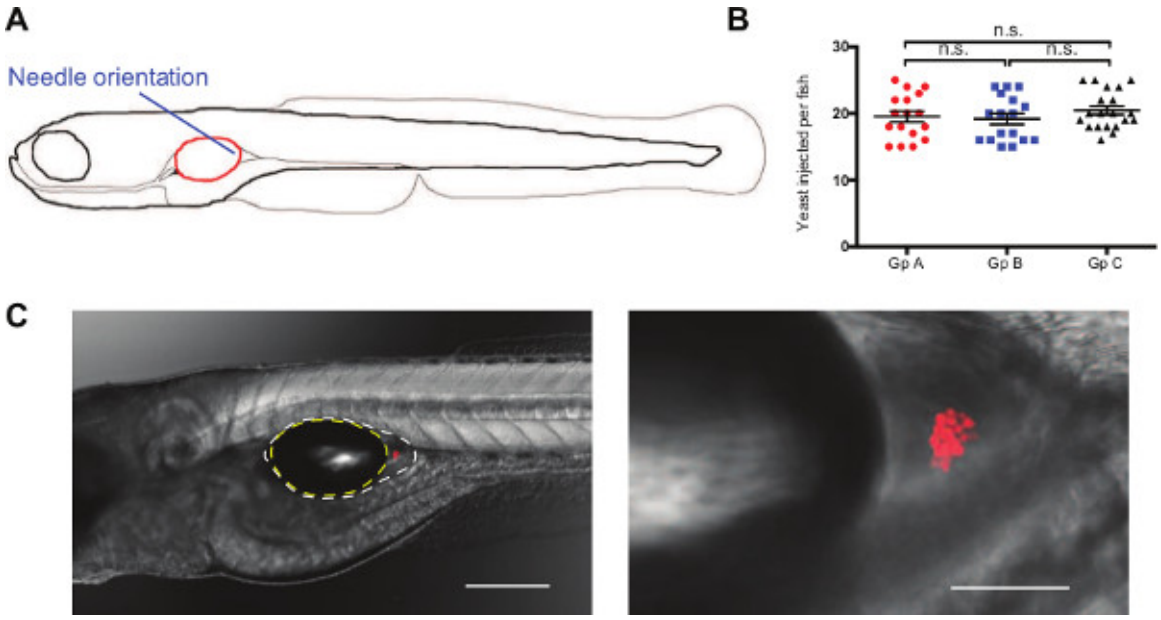

Figure 3: Injection of C. albicans in the swimbladder remains localized to the site of injection. (A) Schematic of the orientation and position of the micro-needle to inject C. albicans into the back of the swimbladder in 4 dpf zebrafish larvae. **(B)** Representative inoculum after selection for injection bolus of 15-25 yeast cells by epifluorescence microscopy for 3 different groups of fish. Mean and standard error of the mean is represented, n = 17, 17, and 20 for groups A, B, and C respectively. **(C)** Representative images of *C. albicans* (Caf2-dTom, red fluorescence expressing Candida) infection in AB juvenile zebrafish immediately after injection. Images were acquired with 10X and 20X objectives (left and right panels, respectively) and are composites of maximum projections in the red channel (12 and 19 slices, respectively) with a single slice in the DIC channel. Outline of the air bubble (yellow) and the epithelial lining (white) are represented on the left panel. Scale bars represent 250 and 50 µm, respectively. Please click here to view a larger version of this figure.

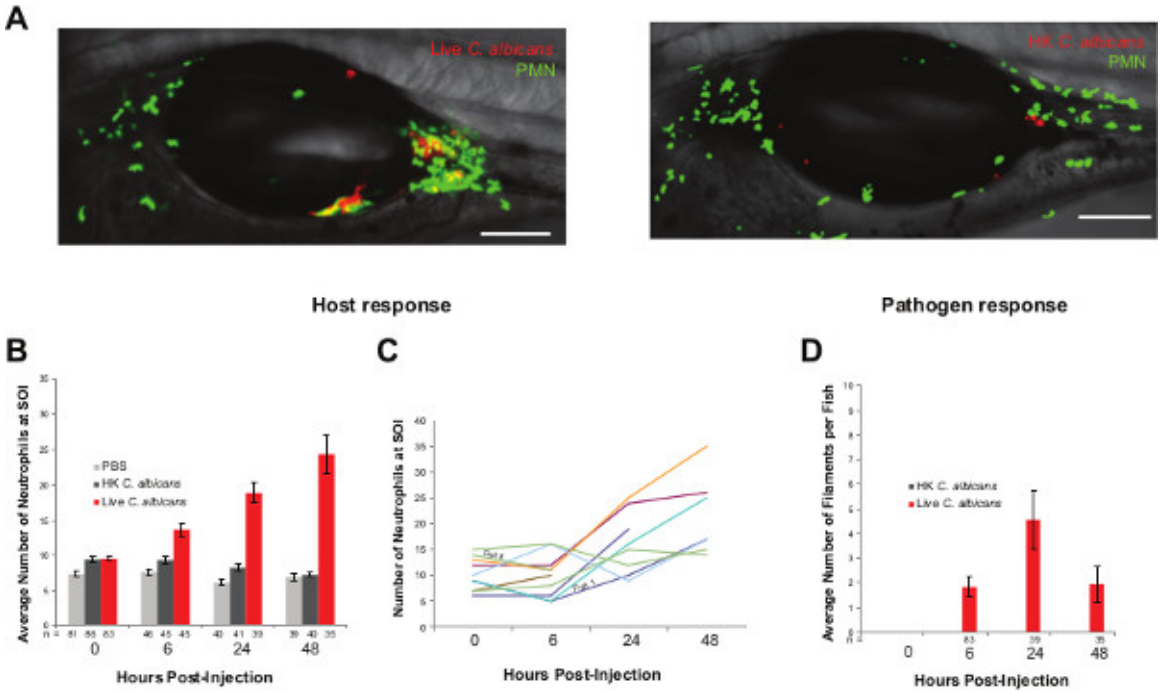

Figure 4: Swimbladder injection allows for spatio-temporal dissection of host pathogen dynamics. (A) Representative images of mpo:GFP fish line injected with live or heat killed (HK) Caf2-dTom in the swimbladder at 4 dpf and imaged 48 hpi. Images are composites of maximum projection on the green and red channels (20 slices) and a single slice in the DIC channel. Scale bars represent 100 µm. **(B,C)**. Host response to *C. albicans* infection. Neutrophils are recruited to the site of infection (SOI) as early as 6 hpi and keep on increasing in number over 48 hr. The possibility to image and keep individual fish separated (24-well plate) allows for detailed immune dynamics to be visualized. **(D)** Pathogen response. *C. albicans* yeast cells are germinating for the first 24 hpi but revert to yeast cells from 24 hpi. Please click here to view a larger version of this figure.

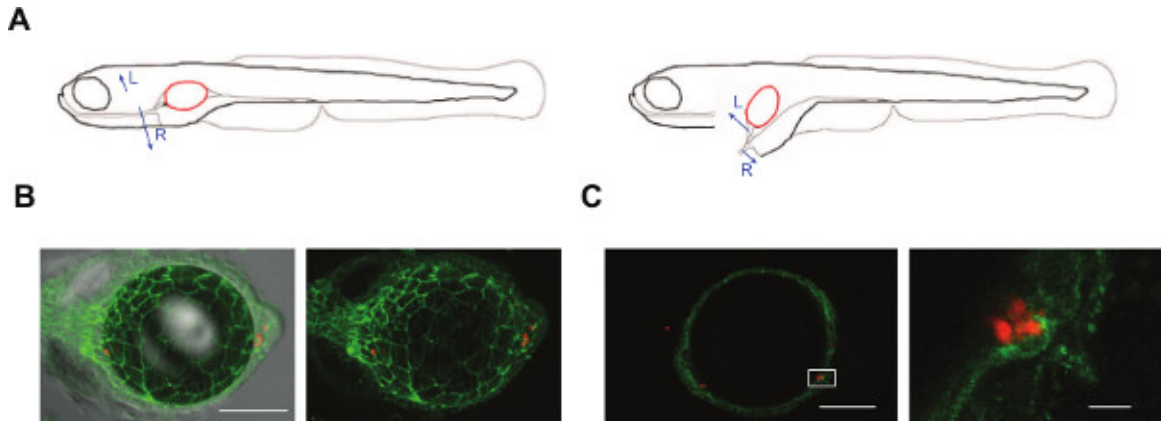

Figure 5: Dissection of the swimbladder allows for finer details to be imaged. (A) Schematic representation of the steps involved in dissection of the swimbladder in 4-5 dpf zebrafish. Blue arrows indicate the direction of pulling with the tweezers (L for Left and R for Right). **(B, C)**. Representative images of dissected swimbladder from α-catenin:citrine fish line[41,42] (green tight junctions) injected at 4 dpf with C. albicans (Caf2-dTom) and imaged by confocal microscopy 2 hpi. Panels are composites of maximum projections in the red and green channels (25 slices for B and 3 slices for C) and a single slice for the DIC in panel B. Scale bars 100 µm in B and 100 µm and 10 µm in C. Please click here to view a larger version of this figure.

Volume (nl)	1	2	3	4	5
Diameter (mm)	0.124	0.156	0.179	0.197	0.212

Table 1: Bolus volume to diameter relationship.

Discussion

Advances and limitations of the swimbladder microinjection disease model

The model presented here is an extension of the mucosal candidiasis immersion model described in Gratacap *et al.* (2013); it adds the advantages of a controlled infection time, a highly reproducible infection dose, and therefore improved efficiency. We demonstrate here new methods that permit non-invasive temporal documentation of infection dynamics in great detail as well as higher resolution *ex vivo* imaging of the swimbladder. These procedures should facilitate the study of *C. albicans*-innate immune system interaction dynamics at the mucosa. A limited number of mucosal infection models have been described in the zebrafish, all limited to digestive tract disturbance/infections[24,43]. The swimbladder model presented here extends the sites of infection to an organ that shares some similarities to the lung and offers a confined site of infection, with less possibility for the pathogen to be washed away.

There are several critical factors that must be taken into account when mastering these techniques. The most important point is the requirement for an inflated swimbladder. This requires the fish to be aged to 5 dpf when reared at 28 °C or 4 dpf at 33 °C. This higher temperature is used to accelerate the development of the fish and better approximate the physiological range of mammalian epithelial temperatures (mouse skin temperature is 33.1 °C[44]). However, the restriction of this model to this particular temperature range needs to be kept in mind and observed phenotypes should be verified in a mammalian system for more complete interpretation. The injection site (the posterior swimbladder) is also critical, as the pneumatic duct remains open in physostomous fish (which includes zebrafish) and high-pressure injection elsewhere in the organ can push the pathogen past the swimbladder and into the digestive tract. Quantification of the inoculum is also less accurate if the yeast cells are not all at the back of the swimbladder, because the thickness of the fish in the trunk makes it difficult to visualize both sides of the swimbladder. Dissection of the swimbladder requires dexterity and imaging needs to take place immediately after to avoid artifacts due to the physical trauma of the procedure.

The limitations of the technique are mainly related to the developmental stage of the fish. This limits the use of morpholino technology to a few days of study, and knockdown efficacy has to be carefully tested to discriminate between full or partial efficacy. Morpholino activity this late in development has been previously reported, and we have also successfully used morpholinos in this model, with validated splice-blocking that was still effective at 5 dpf. The use of pharmacological drugs might be a good alternative in this particular model as there is no restriction for the age of the fish. The use of fish past 72 hr post fertilization sometimes requires more oversight than working with larval zebrafish, depending on the institutional animal care and use committees. The length of study is also constrained, as zebrafish do not survive at high rates for more than 10 days in static laboratory conditions[45]. On the other hand, using juvenile fish of 5 dpf development instead of younger embryos or larvae allows for studies where all organs such as kidneys, liver or pancreas are fully functional[46-49]. Compared to *in vitro* cell culture or *in vivo* murine models, the number of reagents available (antibodies and chemical antagonists-agonists) is limited in the zebrafish; however, the possibility to add chemicals directly to the media is an advantage. The number of knockout and knock-in zebrafish is still limited but the rise of targeted genome editing opens exciting possibilities for the generation of mutants. The combination of the relative ease to construct fluorescent reporter lines (cell type-specific or signaling pathway-specific) with the transparency of the juvenile zebrafish remains one of the primary and unique advantages of this system.

Looking forward

The zebrafish swimbladder infection model extends the range of questions that can be asked about host-pathogen interaction at the vertebrate mucosal epithelium, offering a new route of infection for other pathogens that invade through the epithelium and highlighting the utility of this organ for probing vertebrate disease.

Zebrafish models of epithelial infection at the mucosal level have been published that probe the effects of intestinal tract disturbance by drugs or pathogen[24,43]. However, this mucosal candidiasis model is the first to utilize the swimbladder and thus extends the range of sites of infection that can be investigated in the zebrafish beyond the digestive tract. Differences between the swimbladder mucosal surface and the mammalian lung are not fully elucidated and interpretation/translation of data from this model to higher vertebrate should be made cautiously.

The swimbladder infection fills a current gap in vertebrate infection models and opens up a window for imaging the interactions of innate immune/epithelial cells with a pathogen. Now a diverse range of questions, previously off-limits, is feasible to explore. We can determine the interactions of different innate immune cells with each other and with epithelial cells, their spatio-temporal recruitment, and the nature of *C. albicans* proliferation and morphological switching in relation to immune attack and disease progression in a non-immunosuppressed host. The possibility to image an intact host for several hours to days in great detail represents an obvious and major advantage of this system.

Finally, the ontological and gene expression similarities between the swimbladder and the mammalian lung further suggest that targeting this organ with gene knockdown or chemical drugs may reveal conserved mechanisms of microbial-lung interaction and immunology[50-52].

Disclosures

The authors have nothing to disclose.

Acknowledgements

The authors thank Dr. Le Trinh and Dr. Tobin for generously providing the α-catenin:citrine fish line and Bill Jackman for allowing us to do the filming in his lab. The authors acknowledge the funding sources National Institutes of Health (Grants 5P20RR016463, 8P20GM103423 and R15AI094406) and USDA (Project # ME0-H-1-00517-13). This manuscript is published as Main Agriculture and Forestry Experiment Station publication number 3371.

References

1. Peterson, L. W., & Artis, D. Intestinal epithelial cells: regulators of barrier function and immune homeostasis. *Nat Rev Immunol.* **14** (3), 141–153, doi:10.1038/nri3608, (2014).
2. Elinav, E., Henao-Mejia, J., & Flavell, R. A. Integrative inflammasome activity in the regulation of intestinal mucosal immune responses. *Mucosal Immunol.* **6** (1), 4–13, doi:10.1038/mi.2012.115, (2013).
3. Sansonetti, P. J. To be or not to be a pathogen: that is the mucosally relevant question. *Mucosal Immunol.* **4** (1), 8–14, doi:10.1038/mi.2010.77, (2011).
4. Tlaskalová-Hogenová, H., Stěpánková, R., *et al.* The role of gut microbiota (commensal bacteria) and the mucosal barrier in the pathogenesis of inflammatory and autoimmune diseases and cancer: contribution of germ-free and gnotobiotic animal models of human diseases. *Cell Mol Immunol.* **8** (2), 110–120, doi:10.1038/cmi.2010.67, (2011).
5. Pasparakis, M. Regulation of tissue homeostasis by NF-kappaB signalling: implications for inflammatory diseases. *Nat Rev Immunol.* **9** (11), 778–788, doi:10.1038/nri2655, (2009).
6. Scully, C., el-Kabir, M., & Samaranayake, L. P. Candida and oral candidosis: a review. *Crit Rev Oral Biol Med.* **5** (2), 125–157, doi:10.1177/10454411940050020101, (1994).
7. Reef, S. E., Lasker, B. A., *et al.* Nonperinatal nosocomial transmission of Candida albicans in a neonatal intensive care unit: prospective study. *J Clin Microbiol.* **36** (5), 1255–1259, (1998).
8. Soll, D. R., Galask, R., Schmid, J., Hanna, C., Mac, K., & Morrow, B. Genetic dissimilarity of commensal strains of Candida spp. carried in different anatomical locations of the same healthy women. *J Clin Microbiol.* **29** (8), 1702–1710, (1991).
9. Rindum, J. L., Stenderup, A., & Holmstrup, P. Identification of Candida albicans types related to healthy and pathological oral mucosa. *J Oral Pathol Med.* **23** (9), 406–412, (1994).
10. Mear, J. B., Gosset, P., *et al.* Candida albicans airway exposure primes the lung innate immune response against Pseudomonas aeruginosa infection through innate lymphoid cell recruitment and IL-22 associated mucosal response. *Infect Immun.* **82** (1), 306-315 doi:10.1128/IAI.01085-13, (2013).
11. Faro-Trindade, I., Willment, J. A., *et al.* Characterisation of innate fungal recognition in the lung. *PLoS ONE.* **7** (4), e35675, doi:10.1371/journal.pone.0035675, (2012).
12. Wisplinghoff, H., Bischoff, T., Tallent, S. M., Seifert, H., Wenzel, R. P., & Edmond, M. B. Nosocomial bloodstream infections in US hospitals: analysis of 24,179 cases from a prospective nationwide surveillance study. *Clin Infect Dis.* **39** (3), 309–317, doi:10.1086/421946, (2004).
13. Schaller, M., Zakikhany, K., Naglik, J. R., Weindl, G., & Hube, B. Models of oral and vaginal candidiasis based on in vitro reconstituted human epithelia. *Nat Protoc.* **1** (6), 2767–2773, doi:10.1038/nprot.2006.474, (2006).
14. Weindl, G., Naglik, J. R., *et al.* Human epithelial cells establish direct antifungal defense through TLR4-mediated signaling. *Clin Invest.* **117** (12), 3664–3672, doi:10.1172/JCI28115, (2007).
15. Moyes, D. L., Runglall, M., *et al.* A biphasic innate immune MAPK response discriminates between the yeast and hyphal forms of Candida albicans in epithelial cells. *Cell Host and Microbe.* **8** (3), 225–235, doi:10.1016/j.chom.2010.08.002, (2010).
16. Conti, H. R., Shen, F., *et al.* Th17 cells and IL-17 receptor signaling are essential for mucosal host defense against oral candidiasis. *J Exp Med.* **206** (2), 299–311, doi:10.1084/jem.20081463, (2009).

17. Hise, A. G., Tomalka, J., *et al.* An essential role for the NLRP3 inflammasome in host defense against the human fungal pathogen Candida albicans. *Cell Host Microbe.* **5** (5), 487–497, doi:10.1016/j.chom.2009.05.002, (2009).
18. Gladiator, A. A., Wangler, N. N., Trautwein-Weidner, K. K., & Leibundgut-Landmann, S. S. Cutting Edge: IL-17-Secreting Innate Lymphoid Cells Are Essential for Host Defense against Fungal Infection. *J Immunol.* **190** (2), 521–525, doi:10.4049/jimmunol.1202924, (2013).
19. Hess, I., & Boehm, T. Intravital imaging of thymopoiesis reveals dynamic lympho-epithelial interactions. *Immunity.* **36** (2), 298–309, doi:10.1016/j.immuni.2011.12.016, (2012).
20. Roca, F. J., & Ramakrishnan, L. TNF Dually Mediates Resistance and Susceptibility to Mycobacteria via Mitochondrial Reactive Oxygen Species. *Cell.* **153** (3), 521–534, doi:10.1016/j.cell.2013.03.022, (2013).
21. Tobin, D. M., Vary, J. C., *et al.* The lta4h locus modulates susceptibility to mycobacterial infection in zebrafish and humans. *Cell.* **140** (5), 717–730, doi:10.1016/j.cell.2010.02.013, (2010).
22. Cambier, C. J., Takaki, K. K., *et al.* Mycobacteria manipulate macrophage recruitment through coordinated use of membrane lipids. *Nature.* **505** (7482), 218–222, doi:10.1038/nature12799, (2014).
23. Semova, I., Carten, J. D., *et al.* Microbiota regulate intestinal absorption and metabolism of fatty acids in the zebrafish. *Cell Host and Microbe.* **12** (3), 277–288, doi:10.1016/j.chom.2012.08.003, (2012).
24. Rendueles, O., Ferrières, L., *et al.* A new zebrafish model of Oro-intestinal pathogen colonization reveals a key role for adhesion in protection by probiotic bacteria. *PLoS Pathog.* **8** (7), e1002815, doi:10.1371/journal.ppat.1002815, (2012).
25. Field, H., Ober, E., Roeser, T., & Stainier, D. Formation of the digestive system in zebrafish. I. Liver morphogenesis. *Dev Biol.* **253** (2), 279–290, (2003).
26. Field, H., Dong, P., Beis, D., & Stainier, D. Formation of the digestive system in zebrafish. II. Pancreas morphogenesis. *Dev Biol.* **261** (1), 197–208, doi:10.1016/S0012-1606(03)00308-7, (2003).
27. Sullivan, L., Daniels, C., Phillips, I., Orgeig, S., & Whitsett, J. Conservation of surfactant protein A: evidence for a single origin for vertebrate pulmonary surfactant. *J Mol Evol.* **46** (2), 131–138, doi:10.1007/PL00006287, (1998).
28. Oehlers, S. H., Flores, M. V., Chen, T., Hall, C. J., Crosier, K. E., & Crosier, P. S. Topographical distribution of antimicrobial genes in the zebrafish intestine. *Dev Comp Immunol.* **35** (3), 385–391, doi:10.1016/j.dci.2010.11.008, (2011).
29. Winata, C., Korzh, S., Kondrychyn, I., Zheng, W., Korzh, V., & Gong, Z. Development of zebrafish swimbladder: The requirement of Hedgehog signaling in specification and organization of the three tissue layers. *Dev Biol.* **331** (2), 222–236,doi: 10.1016/j.ydbio.2009.04.035, (2009).
30. Zheng, W., Wang, Z., Collins, J. E., Andrews, R. M., Stemple, D., & Gong, Z. Comparative transcriptome analyses indicate molecular homology of zebrafish swimbladder and mammalian lung. *PLoS ONE.* **6** (8), e24019, doi:10.1371/journal.pone.0024019.t002, (2011).
31. Galuppi, R., Fioravanti, M., Delgado, M., Quaglio, F., Caffara, M., & Tampieri, M. Segnalazione di due casi do micosi della vescica natatoria in Sparus aurata e Carrassius auratus. *Bollettino Societa Italiana di Patologic.* **32**, 26–34 (2001).
32. Gratacap, R. L., Rawls, J. F., & Wheeler, R. T. Mucosal candidiasis elicits NF-κB activation, proinflammatory gene expression and localized neutrophilia in zebrafish. *Dis Model Mech.* **6** (5), 1260–1270, doi:10.1242/dmm.012039, (2013).
33. Brothers, K. M., Gratacap, R. L., Barker, S. E., Newman, Z. R., Norum, A., & Wheeler, R. T. NADPH oxidase-driven phagocyte recruitment controls Candida albicans filamentous growth and prevents mortality. *PLoS Pathog.* **9** (10), e1003634, doi:10.1371/journal.ppat.1003634, (2013).
34. Rosen, J. N., Sweeney, M. F., & Mably, J. D. Microinjection of zebrafish embryos to analyze gene function. *Journal of visualized experiments : JoVE.* (25), doi:10.3791/1115 (2009).
35. Anaissie, E. J., & Bodey, G. P. Fungal infections in patients with cancer. *Pharmacotherapy.* **10** (6 (Pt 3)), 164S–169S, (1990).
36. Fidel, P. L., Barousse, M., *et al.* An intravaginal live Candida challenge in humans leads to new hypotheses for the immunopathogenesis of vulvovaginal candidiasis. *Infect Immun.* **72** (5), 2939–2946, doi: 10.1128/IAI.72.5.2939-2946.2004, (2004).
37. Akova, M., Akalin, H. E., *et al.* Efficacy of fluconazole in the treatment of upper gastrointestinal candidiasis in neutropenic patients with cancer: factors influencing the outcome. *Clin Infect Dis.* **18** (3), 298–304, doi: 10.1093/clinids/18.3.298, (1994).
38. Farah, C. S., Elahi, S., *et al.* T cells augment monocyte and neutrophil function in host resistance against oropharyngeal candidiasis. *Infect Immun.* **69** (10), 6110–6118, doi:10.1128/IAI.69.10.6110-6118.2001, (2001).
39. Renshaw, S. A., Loynes, C. A., Trushell, D. M. I., Elworthy, S., Ingham, P. W., & Whyte, M. K. B. A transgenic zebrafish model of neutrophilic inflammation. *Blood.* **108** (13), 3976–3978, doi:10.1182/blood-2006-05-024075, (2006).
40. Kanther, M., Sun, X., *et al.* Microbial Colonization Induces Dynamic Temporal and Spatial Patterns of NF-κB Activation in the Zebrafish Digestive Tract. *Gastroenterology.* **141** (1), 197–207, doi:10.1053/j.gastro.2011.03.042, (2011).
41. Trinh, L. A., Hochgreb, T., *et al.* A versatile gene trap to visualize and interrogate the function of the vertebrate proteome. *Genes Dev.* **25** (21), 2306–2320, doi:10.1101/gad.174037.111, (2011).
42. Trinh, L. A., Fraser, S. E., & Moens, C. B. Zebrafish Neural Tube Morphogenesis Requires Scribble-Dependent Oriented Cell Divisions. *Curr Biol.* **21** (1), 79–86, doi:10.1016/j.cub.2010.12.005, (2011).
43. Oehlers, S. H. B., Flores, M. V., *et al.* Expression of zebrafish cxcl8 (interleukin-8) and its receptors during development and in response to immune stimulation. *Dev Comp Immunol.* **34** (3), 352–359, doi:10.1016/j.dci.2009.11.007, (2010).
44. Bast, D. J., Yue, M., *et al.* Novel murine model of pneumococcal pneumonia: use of temperature as a measure of disease severity to compare the efficacies of moxifloxacin and levofloxacin. *Antimicrob Agents Chemother.* **48** (9), 3343–3348, doi:10.1128/AAC.48.9.3343-3348.2004, (2004).
45. Davis, J., Clay, H., Lewis, J., Ghori, N., Herbomel, P., & Ramakrishnan, L. Real-time visualization of mycobacterium-macrophage interactions leading to initiation of granuloma formation in zebrafish embryos. *Immunity.* **17** (6), 693–702, doi:10.1016/S1074-7613(02)00475-2, (2002).
46. Pack, M., Solnica-Krezel, L., *et al.* Mutations affecting development of zebrafish digestive organs. *Development.* **123**, 321–328, (1996).
47. Le Guyader, D., Redd, M. J., *et al.* Origins and unconventional behavior of neutrophils in developing zebrafish. *Blood.* **111** (1), 132–141, doi:10.1182/blood-2007-06-095398, (2008).
48. Kimmel, C. B., Ballard, W. W., Kimmel, S. R., Ullmann, B., & Schilling, T. F. Stages of embryonic development of the zebrafish. *Dev Dyn.* **203** (3), 253–310, doi:10.1002/aja.1002030302, (1995).
49. Parichy, D. M., Elizondo, M. R., Mills, M. G., Gordon, T. N., & Engeszer, R. E. Normal table of postembryonic zebrafish development: staging by externally visible anatomy of the living fish. *Dev Dyn.* **238** (12), 2975–3015, doi:10.1002/dvdy.22113, (2009).
50. Noverr, M. C., & Huffnagle, G. B. Does the microbiota regulate immune responses outside the gut? *Trends in Microbiology.* **12** (12), 562–568, doi:10.1016/j.tim.2004.10.008 (2004).
51. Huffnagle, G. B. The microbiota and allergies/asthma. *PLoS Pathog.* **6** (5), e1000549, doi:10.1371/journal.ppat.1000549, (2010).

52. Kim, Y.-G., Udayanga, K. G. S., Totsuka, N., Weinberg, J. B., Núñez, G., & Shibuya, A. Gut dysbiosis promotes M2 macrophage polarization and allergic airway inflammation via fungi-induced PGE_2. *Cell Host Microbe.* **15** (1), 95–102, doi:10.1016/j.chom.2013.12.010, (2014).